Historic Flow Conditions Preserved in Siliceous Sinter Vent Walls of Three Newly-Exposed Hot Spring Vents at Orakei Korako, New Zealand.

Bridget Y. Lynne[1,2]

[1]University of Auckland, 70 Symonds St, Auckland, New Zealand

[2]Geothermal Scientific Investigations Ltd, 11 Kyle Rd, Greenhithe, Auckland, New Zealand

b.lynne@auckland.ac.nz or bridget.lynne@gsilimited.com

Keywords: *Reactivation of buried hot spring vents, changes to surface activity, Orakei Korako, Ground Penetrating Radar, Scanning Electron Microscopy, siliceous sinter textures.*

ABSTRACT

Orakei Korako geothermal field is located in the Taupo Volcanic Zone, New Zealand, and is a protected geothermal system. In 2012, a Ground Penetrating Radar (GPR) survey, combined with a 1.5 m deep temperature probe survey was undertaken around the boardwalk at Orakei Korako. In 2019, following a small hydrothermal eruption, three new vents appeared at a site that was mapped in 2012 by GPR and downhole temperature measurements. Vent walls in each of the new vents expose a variety of siliceous sinter textures. In 2019, samples were collected from each vent and examined using Scanning Electron Microscopy (SEM) to determine paleo-hydrological and paleo-environmental conditions that occurred at the time the sinter formed. SEM observations determined all three vents were dominated by mid-temperature alkali chloride water (35-59 °C). Pristine microbial preservation within the sinter samples indicates one vent would have been a quiet pool with minimal water movement and overflow, while the other two vents would have had a higher discharge rate. Post-depositional dissolution textures were also documented in samples from two of the vents. Examination of the preserved sinter textures has enabled paleo-flow conditions to be identified, reconstruction of historic hot spring settings to be established and shown more recently, evidence of post-depositional over-printing via acidic steam condensate.

1. INTRODUCTION

Orakei Korako geothermal field is a protected geothermal system and a popular tourist site. It is located approximately 25 km northeast of Taupo, within the Taupo Volcanic Zone, New Zealand (Fig. 1). The geothermal field straddles the Waikato River with most of the surface activity located on the eastern side of the river. Thermal activity is dominated by alkali chloride features, typically hot springs, hot pools and expansive siliceous sinter terraces. Siliceous sinters form from discharging silica-rich, alkali chloride hot spring water. As the water discharges and cools to below 100 °C, silica precipitates and accumulates to form hot spring rocks referred to as siliceous sinter (Fournier and Rowe, 1966; Fournier, 1985; Williams and Crerar, 1985). Silica deposits on everything the thermal water flows over, including living microbial mats that thrive in the warm discharging water. Eventually the rate of silica deposition is more rapid than microbial growth and they become entombed in silica and silicified. The silicification process captures and preserves evidence of former viable microbial mats and their associated hydrothermal conditions, such as water temperature and flow rate, at the time they became silicified (Cady and Farmer, 1996; Lynne, 2012).

Documented geothermal surface activity at Orakei Korako dates back to the 1800's (Allen, 1894; Hochstetter, 1867). More recently, Lloyd (1972), Hamlin (1999) and Howe and Lynne (2010) documented the active surface activity. Dating of the historic sinter outcrops in the area indicates alkali chloride fluids have discharged in the area for at least six thousand years (Campbell et al., 2001; Campbell and Lynne, 2006).

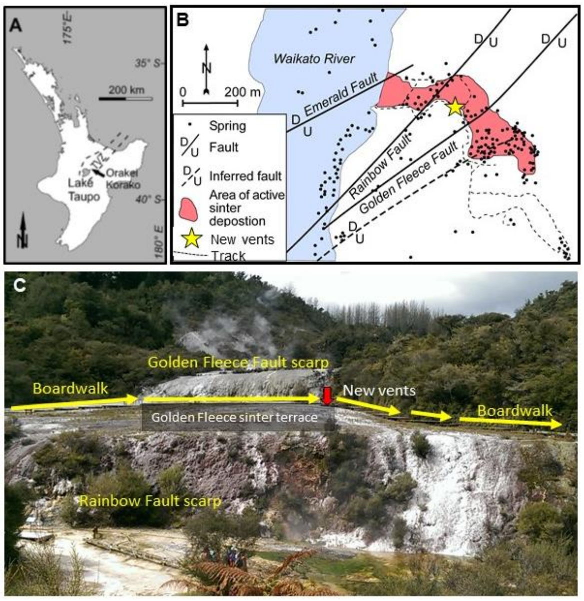

Figure 1: Location of new vents exposed in 2019 at Orakei Korako geothermal field, Taupo Volcanic Zone, North Island of New Zealand.

In 2012, a Ground Penetrating Radar (GPR) survey was undertaken over an area (Lynne and Smith, 2020), that in 2019 experienced a small hydrothermal eruption. The eruption exposed three small hot spring vents and was observed by the staff at Orakei Korako, who retold the event as a small steam eruption.

The 2012 GPR survey undertaken at the site of the 2019 hydrothermal eruption revealed low-amplitude reflections indicating intense hydrothermal alteration to approximately 1 m below the surface (Fig. 2). However, there was no indication at the surface, of buried vents. The 2012 GPR survey was coupled with a 1.5 m deep temperature probe survey which revealed 100 °C at 0.5 m depth. In 2012, there was no discharging steam or evidence of heat at the surface. Results of the 2012 survey were presented at the 2020 New Zealand Geothermal Workshop (Lynne and Smith, 2020).

Site visits soon after the eruption in 2019 revealed all three vents were active. Hot water was visible in the base of the West and North vents and steam discharged from the East vent (Fig. 3). Mild and intermittent wafts of hydrogen sulphide gas could be smelt in the area. A recent site visit in August 2022, confirmed these vents have changed little since 2019 and are still active.

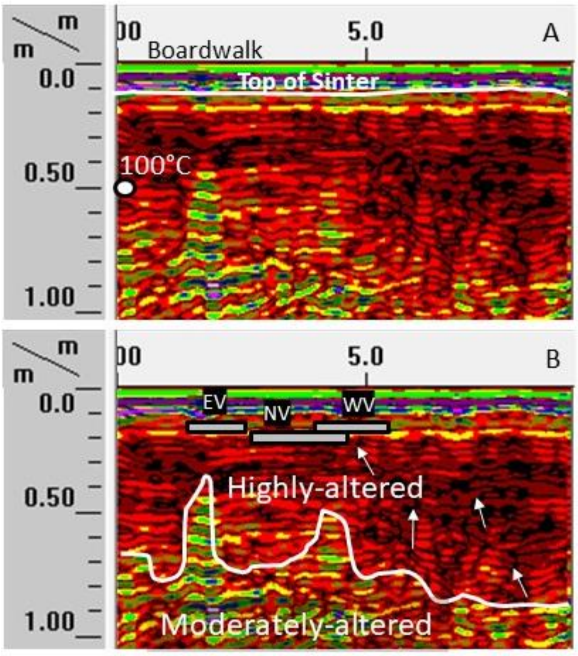

Figure 2: 2012 GPR image collected along boardwalk at site of new vents before they were exposed. (A) Low-amplitude reflections (red areas) indicate highly-altered subsurface. Medium amplitude reflections (yellow and green areas) indicate moderately-altered subsurface. 0.1 m air gap between the boardwalk and top of the sinter terrace is shown as multi-coloured, continuous horizontal lines. Downhole temperature at 0.5 m depth measured 100°C (white circle). (B) Newly-exposed East vent (EV), North vent (NV) and West vent (WV) are located in the highly-altered GPR signature area. Contorted fracture pathways in highly-altered subsurface (arrows).

The three 2019 newly-exposed hot spring vents display a variety of siliceous sinter textures. These textures indicate paleo-flow rates and water temperature of the once discharging hot springs. Sinter samples from the vent walls were sampled and analysed under a Scanning Electron Microscope (SEM) with results documented in this study. Sinter textures observed within each vent have been paired with a photograph of the modern-day equivalent, as they occurred on the sinter terraces at Orakei Korako in 2019.

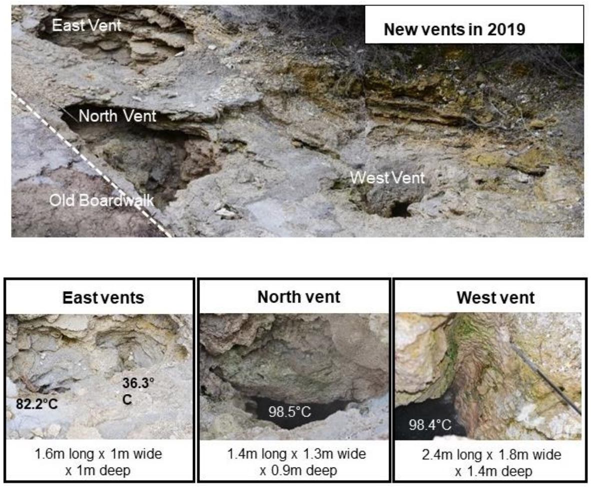

Figure 3: East, West and North vents exposed in 2019.

2. METHODS

Scanning Electron Microscopy (SEM) was used to observe all biotic and abiotic components preserved within sinter samples collected from the walls of each vent. Samples were mounted on aluminium stubs using epoxy. The stubs were coated with platinum using a high-resolution Polaron SC7640 sputter coater. SEM operating conditions were 20 keV accelerating voltage and a working distance of 10 mm. The SEM is housed at the University of Auckland.

The GPR unit used in 2012 was a GSSI SIR-2000 with a GSSI 200 MHz antenna. Settings included continuous run mode, a range of 200 ns, and a dielectric constant of 6 along the boardwalk.

3. RESULTS

3.1 West vent

Three sinter textures observed in the West vent are referred to as bubble-mat, streamer and flow-back textures (Fig. 4).

The uppermost 0.2 m of the western side of the vent displays elongated bubble-mat, sinter texture. Living microbial mats that form this texture represent mid-temperature (35-59 °C) flowing water. These microbes are photosynthesizing, releasing oxygen which becomes trapped in the gel-like mat and creates bubbles. These bubbles become elongated as they are stretched to accommodate the velocity of the flowing water. In hand specimen, silicified bubble-mat texture comprises of stacked, thin, shell-like sinter platelets with elongated oval voids separating the thin platelets.

Streamer textures were observed around the western side of the vent, near the surface. Streamer textures represent microbes that grow parallel to the flow direction. They do not indicate specific water temperature but do indicate fast flowing water.

Flow-back textures form as water from the surface flows back down into the vent. Flow-back texture is visible down the eastern and southern sides of the vent, covering underlying sinter textures. As flow-back texture is visible for 1 m into the vent, this suggests the water level of the vent remained at least 1 m below the surface for some considerable time.

The flow-back texture was sampled at 0.5 m into the vent. SEM observations indicate: (1) Multiple vertically-aligned ridges parallel to the flow of the water back into the vent, (2) Mid-temperature (35-59 °C) sized microbial filaments with

ISSN2703-4275

total exterior diameters of <2 µm, and (3) Moderate dissolution of some of the microbial filaments (Fig. 5).

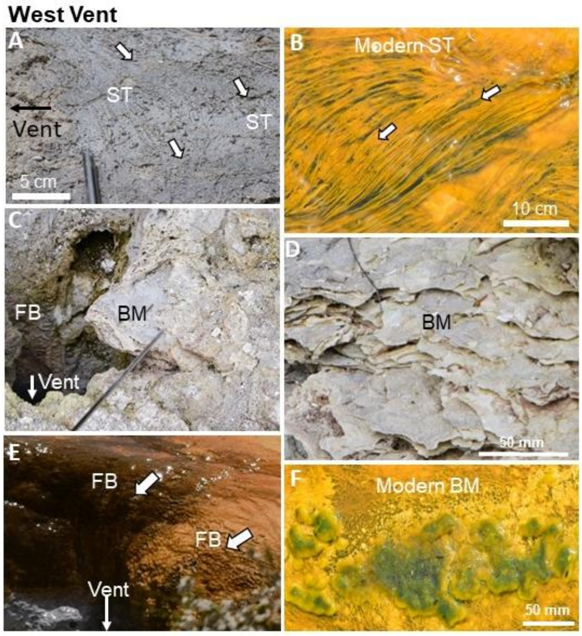

Figure 4: West vent. (A) Streamer texture (ST). (B) Living streamer microbial mat. (C) Flow-back (FB) and bubble-mat (BM) textures. (D) Bubble-mat texture with thin silica plates and oval voids. (E) Present-day setting showing flow-back texture. (F) Living bubble-mat microbial mats.

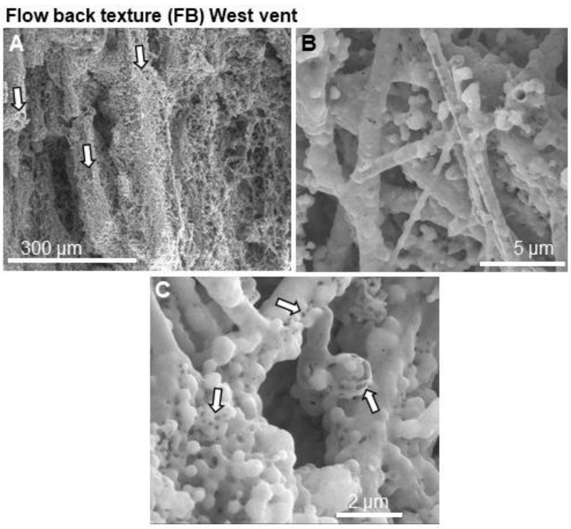

Figure 5: SEM images of the flow-back sinter texture from the West vent. (A) Vertical ridges. (B) Clusters of mid-temperature sized microbial filaments (<2 µm total exterior diameter). (C) Mild dissolution textures shown as holes or pitted surfaces (arrows) on both opal-A silica spheres and microbial filament sheaths.

3.2 North vent

The walls of the North vent exposed three distinct sinter textures; conical tufted, bubble-mat and nodular texture (Fig. 6).

At approximately 0.5 m depth and on the eastern side of the vent, conical tufted texture is visible. Conical tufted microbial mats commonly thrive in calm, ponded, mid-temperature hot spring water bodies (35-59 °C), where there is very little water movement (Fig. 6).

Circular bubble-mat textures are present on the western side of the vent at a 0.5 m depth. Living microbes that form circular bubble-mat textures thrive in mid-temperature water (35-59 °C) where there is minimal or slow flow. Overlying these textures is elongated bubble-mat sinter representing silicified microbes that would have inhabited mid-temperature water that was flowing faster than where the circular bubble-mats formed (Fig. 6).

Near the base, on the western side of the vent and at 0.6 m into the vent, nodular texture is visible. SEM examination of the nodular area revealed mid-temperature microbes dominate this sinter. Dissolution textures are also visible in the mid-section of this sample, indicating post-depositional overprinting by acidic steam condensate (Figs. 7 and 8).

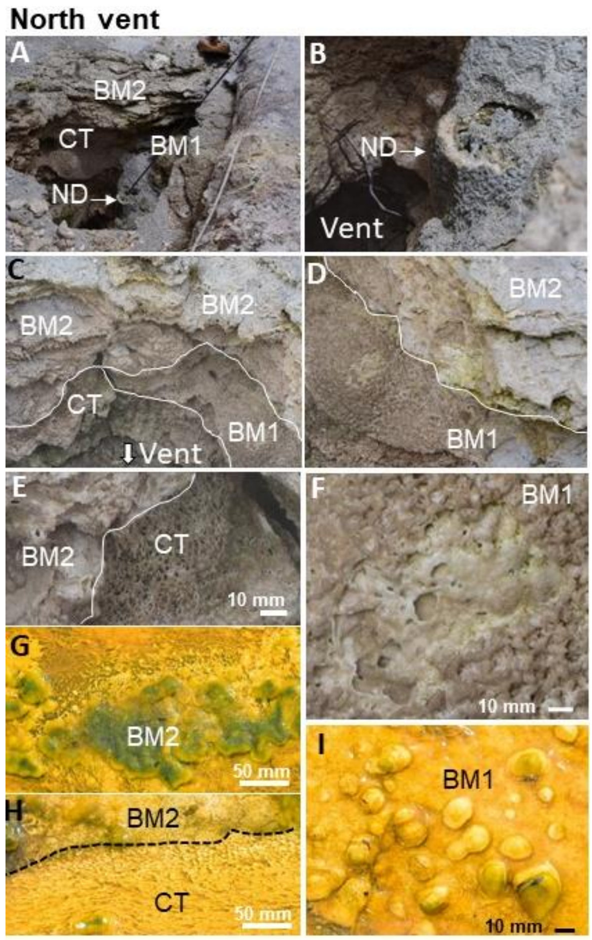

Figure 6: North vent. (A-F) Elongated bubble-mat (BM2), circular bubble-mat (BM1), conical tufted (CT) and nodular (ND) sinter textures exposed in vent. (G-I) Modern-day, living microbial mats. Elongated bubble-mat (BM2), circular bubble-mat (BM1 and conical tufted mat (CT).

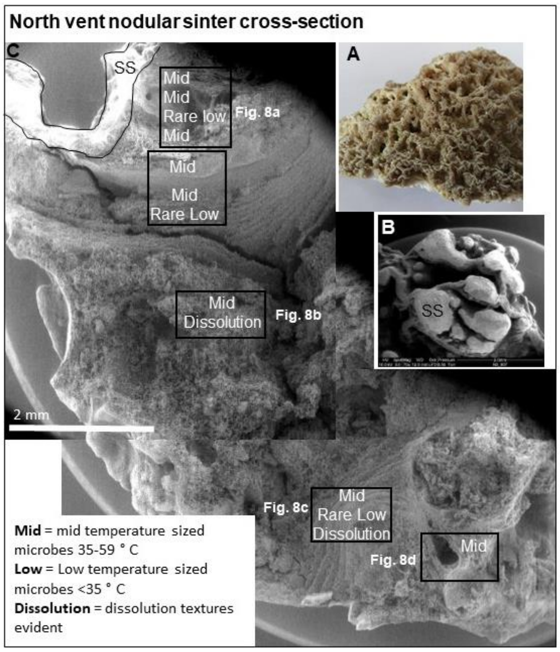

Figure 7: Nodular sinter in North vent. (A) Hand specimen photograph. (B-C) SEM images. (B) Exterior smooth surfaces of nodules (ss). (C) Cross-section of nodular sinter with exterior smooth silica rim (ss).

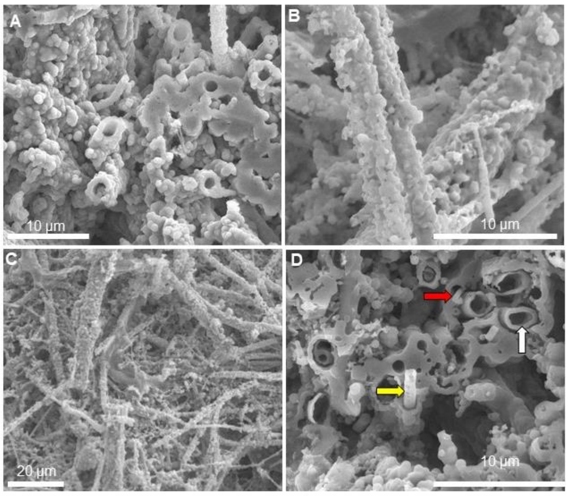

Figure 8: Preservation of mid-temperature sized filamentous identified in Figure 7. (A) Microbial preservation and opal-A spheres. No dissolution. (B-C) Dissolution of mid-temperature silicified microbes shown as melted opal-A spheres (B) and etched and pitted surfaces of filamentous microbes (B and C). (D) Hollow microbial sheaths (white arrow), unaltered microbial trichome (red arrow) and microbial trichome with pitted dissolution textures (yellow arrow).

3.3 East vent

The East Vent consists of alternating layers of conical tufted and elongated bubble-mat sinter textures with preserved plant material around the top of the vent (Fig. 9).

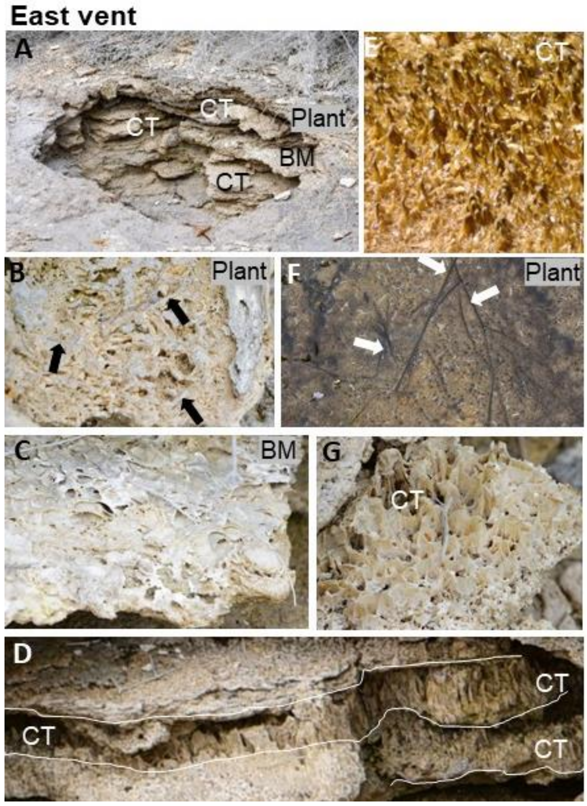

Figure 9: East vent. (A) Overview of preserved bubble-mat (BM), conical tufted (CT) sinter textures and plant material. (B) Silicified plant material (arrows). (C) Bubble-mat texture (BM). (D and G) Conical tufted texture (CT). (E) Living conical tufted microbial mat. (F) Modern setting with plant material in hot spring discharge channel.

3.4 Historic hot spring conditions and post-depositional over-printing

Sinter samples from all three vent walls are dominated by silicified, mid-temperature sized, filamentous microbes. This indicates the temperature of the discharging hot springs was mostly between 35-59 °C. However, based on the microbial preservation, there are differences between the three vents with regards to hot spring environmental conditions. The East vent would have been a quiet pool with minimal water movement, as inferred from the preservation of the conical tufted sinter texture. The North and West vents, which are dominated by bubble-mat sinter texture suggest these pools had a higher flow rate compared to the East vent. Post-depositional over-printing of the sinter in the vent walls is revealed by the pitted surfaces in samples from the North and West vents. Stratigraphic columns of the sinter textures and associated hot spring conditions for each vent and sites of post-depositional acidic steam condensate over-printing are shown in Figure 10.

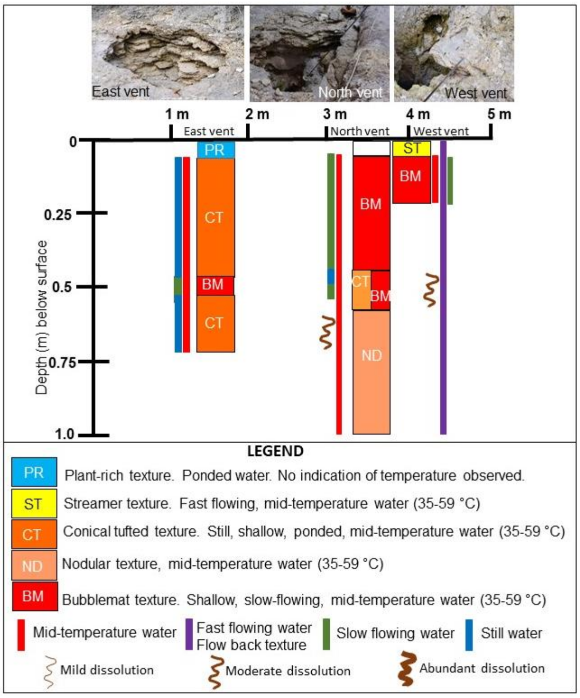

Figure 10: Stratigraphic columns of the East, North and West vents. Siliceous sinter textures, the depths at which they were identified and associated sinter formation hot spring environmental conditions and post-depositional processes.

3.5 Shallow subsurface temperature measurements

In 2019, eight near-surface, downhole temperature measurements revealed subsurface temperatures ranged from 21 to 61 °C, at depths as shallow as 10 mm to 100 mm, respectively (Fig. 11). Hard subsurface conditions prevented the temperature probe form penetrating the ground deeper than those depths recorded. A new boardwalk now bypasses the area where the newly-exposed vents appeared (Fig. 11).

Figure 11: 2019 near-surface, measured temperatures in area underneath the old boardwalk (white dotted line) and over the new North vent (NV) and beside the new West vent (WV) and new East vent (EV). Measured temperature/depth of measurement shown for each location (red dot).

4. DISCUSSION

4.1 Microbial preservation infers hot spring paleo-environmental conditions

Preservation of silicified microbes in three newly-exposed vents at Orakei Korako geothermal field have recorded the paleo-hydrological and paleo-environmental hot spring conditions. SEM examination of selected sinter samples reveal the North and West vent formed under similar conditions. These two vents would have had water discharging from their vents that was between 35 and 59 °C. The water would have been flowing but shallow, as indicated by the dominance of bubble-mat sinter textures. The East vent would have also been discharging water between 35 and 59 °C. However, this hot spring would have been a quiescent pool as indicated by the dominance of conical tufted sinter textures that thrive in still water bodies.

4.2 Dissolution via acidic steam condensate overprinting

Moderate dissolution textures were identified via SEM imaging at 0.5 m in the West vent and 0.7 m in the North vent. The downhole temperature survey showed temperatures as high as 61 °C at 100 mm depth, adjacent to the North and West vents. These higher than ambient temperatures suggest active hydrothermal alteration processes are in play. The dissolution textures observed are typical of acidic steam condensate over-printing siliceous sinter (Lynne et al., 2008, 2017; Lynne and Smith, 2013). The measured subsurface temperatures, indicating heat in the shallow subsurface, also support acidic steam condensate post-depositional process are altering the sinter. GPR results provide further evidence of subsurface hydrothermal processes as shown by the area of low-amplitude reflections rimmed by higher-amplitude reflections. Low-amplitude reflections such as those identified at the new vent sites have also been reported at Yellowstone National Park, USA on a sinter terrace where the sinter was actively being over-printed with acidic steam condensate (Lynne et al., 2017). The Yellowstone sinter hydrothermal alteration mirrors the situation at these three newly-exposed Orakei Korako vents.

4.3 Changes over time

A four-step time sequence has been observed at the newly-exposed Orakei Korako vents; (1) Hot pools that discharged mid-temperature (35-59 °C) water depositing silica to form siliceous sinter hot spring rock and silicifying microbial communities, (2) Post-depositional acidic steam condensate over-printing of the sinter, (3) Exposure of the new vents through a hydrothermal eruption, and (4) Present-day hot pools that are not overflowing.

The changing nature of geothermal activity is not uncommon in geothermal settings. Lloyd (1972) thoroughly mapped the location of all active thermal features at Orakei Korako and there is no mention of these vents in his report. The next step is to date the plant-rich sinter exposed in these vents.

ACKNOWLEDGEMENTS

We would like to thank Craig and Philippa Gibson for allowing on-going access to Orakei Korako and the University of Auckland for supporting this research.

REFERENCES

Allen, G.F.: Willis's Guide Book of New Route for Tourists, Auckland-Wellington via the Hot Springs, Taupo, the Volcanoes and the Wanganui River. Willis, Wanganui. 200 pp. (1894).

Cady, S.L., and Farmer, J.D.: Fossilization processes in siliceous thermal springs: trends in preservation along thermal gradients. In: Bock, G.R., Goode, J.A. (Eds.), Evolution of Hydrothermal Ecosystems on Earth (and Mars?). *Proceedings of the CIBA Foundation Symposium*. *volume 202,* Wiley, Chichester, U.K., pp. 150-173. (1996).

Campbell, K.A., and Lynne, B.Y.: Diagenesis and dissolution at Sinter Island (456 years BP), Taupo Volcanic Zone: Silica stars and the birth of quartz. *28th New Zealand Geothermal Workshop,* New Zealand. (2006).

Campbell, K.A., Sannazzaro, K., Rodgers, K.A., Herdianita, N.R., Browne, P.R.L.: Sedimentary facies and mineralogy of the Late Pleistocene Umukuri silica sinter, Taupo Volcanic Zone, New Zealand. *Journal of Sedimentary Research,* volume 71, pp. 728-747. (2001).

Fournier, R.O.: The behaviour of silica in hydrothermal solutions. *Reviews in Economic Geology,* volume 2, pp. 45-62. (1985).

Fournier, R.O., and Rowe, J.J..: Estimation of underground temperatures from the silica content of water from hot springs and steam wells. *American Journal of Science*, volume 264, pp. 685–697. (1966).

Hamlin, K.: Geological studies of the Orakeikorako geothermal field, Taupo Volcanic Zone, New Zealand. *Unpublished Thesis, University of Auckland.* 118 pp. (1999).

Hochstetter, F. von.: New Zealand. Cotta, Stuttgart. 515 pp. (1867).

Howe, T., and Lynne, B.Y.: Changes in hot spring activity at Orakei Korako: the last 50 years. *32nd New Zealand Geothermal Workshop,* New Zealand. (2010).

Lloyd, E.F.: Geology and hot springs of Orakei Korako. *New Zealand Geological Survey,* Bulletin 85, 164 pp. (1972).

Lynne, B.Y.: Mapping vent to distal-apron hot spring paleo-flow pathways using siliceous sinter architecture. *Geothermics,* volume 43, pp. 3-24. (2012).

Lynne, B.Y., and Smith, G.J.: Three new hot spring vents exposed at Orakei Korako Geothermal Field, New Zealand. *42nd New Zealand Geothermal Workshop,* Waitangi, New Zealand. (2020).

Lynne, B.Y., and Smith, G.J.: A new investigative approach to understanding heat migration pathways within the shallow subsurface at Orakei Korako, New Zealand. *Geothermal Resource Council Transactions,* USA, volume 37. (2013).

Lynne, B.Y., Campbell, K.A., Moore, J.N., Browne, P.R.L.: Origin and evolution of the Steamboat Springs siliceous sinter deposit, Nevada, USA. *Sedimentary Geology,* volume 210, pp. 111-131. (2008).

Lynne, B.Y., Heasler, H., Jaworowski, C., Foley, D., Smith, I.J., Smith, G.J.: Using Ground Penetrating Radar, scanning electron microcopy and thermal infrared imagery to document near-surface hydrological changes in the Old Faithful Geyser area, Yellowstone national Park, USA. *Geothermics,* volume 68, pp. 33-53. (2017).

Lynne, B.Y., Heasler, H., Jaworowski, C., Smith, G.J., Smith, I.J., Foley, D.: Ground Penetrating Radar documents short-term near-surface hydrological changes around Old Faithful Geyser Yellowstone National Park, USA. *Journal of Volcanology and Geothermal Research,* volume 354, pp. 1-12. (2018).

Williams, L.A., and Crerar, D.A.: Silica diagenesis, II: general mechanisms. *Journal of Sedimentary Petrology,* volume 55, pp. 312–321. (1985).